JOURNAL OF Applied Polymer SCIENCE

# Combination of temperature and saturated vapor annealing for phase separation of block copolymer

**Jan Švanda, Oleksiy Lyutakov, Vladimíra Vosmanská, Václav Švorčík**
Department of Solid State Engineering, Institute of Chemical Technology, Prague 166 28, Czech Republic
Correspondence to: O. Lyutakov (E-mail: lyutakoo@vscht.cz)

**ABSTRACT:** Phase separation of block copolymer films is a perspective technique for the creation of nanostructured templates. The phase separation can be induced by thermal or vapor solvent annealing. However, a standardized and reproducible technique of the phase separation is still missing, even though many papers describing various experimental conditions. In this article we have tried to develop standardized and reproducible technique of the phase separation, which can be easily scaled up. For this purpose we used the combination of the thermal and vapor annealing of poly(styrene-b-4-vinylpyridine) copolymer films on a glass substrate under static conditions. The technique was tailored by the choice of optimal solvent for the vapor annealing, based on the solvent–polymer interaction. Finally, the films were reconstructed by immersing in methanol or ethanol and stretching of the P4VP component during the reconstruction was investigated by the angle-resolved X-ray photoelectron spectroscopy. Morphology of the films was investigated by the atomic force microscopy and confocal microscopy. The kinetics of the phase separation was also studied. The presented combined technique of the thermal and vapor annealing can be easily temperature-controlled for reproducibly obtaining the films of a desired morphology. © 2014 Wiley Periodicals, Inc. J. Appl. Polym. Sci. **2015**, *132*, 41853.

**KEYWORDS:** coatings; copolymers; films; morphology; nanostructured polymers

Received 13 August 2014; accepted 6 December 2014
**DOI: 10.1002/app.41853**

## INTRODUCTION

Modern photonics and electronics tend to move into nanoscale and effective tools for the creation of nanostructures on large surface areas are needed. Advanced techniques such as electron beam writing or two-photon lithography are perspective for production of specific nanostructures with various dimensions and shapes, but their application on the formation of ordered systems of nanoobjects on the large area is irrational. The periodical arrays of structures can be easily produced from initially homogeneous polymer thin films by applying external treatment, such as electric fields,[1,2] mechanical action,[3,4] temperature gradients,[5,6] chemical patterning,[7,8] laser treatment,[9,10] and so on.

The phase separation of block copolymers (BCPs) is also a suitable approach for the creation of patterned polymer templates.[11,12] During the phase separation, the BCPs spontaneously generate highly ordered structures with nanometer precision over a large area, simply and cost-effectively. The dimension of BCP-based depends on the length of copolymer blocks and their orientation (symmetry). The quality of formed nanostructures is a function of the annealing parameters. Morphologies such as spheres, cylinders, continuous interpenetrating network-like structures, lamellae, and combinations of these features are formed depending on the technological procedure of the BPCs.[11,12] Thus, orientation and lateral ordering of the microdomains in the BCPs is one of the most important issues. The periodical pattern can be prepared by the annealing in solvent vapor, temperature annealing or directly during spin-coating deposition from selective solvent mixtures.[12–14] In the case of the solvent vapor annealing, there are several key issues which influence the resulting morphology: choice of the suitable solvent,[11–18] method of solvent annealing (static or dynamic), applied temperature,[19] duration of solvent treatment, substrate[7] and film thickness.[20,21]

The resulting orientation of the nanodomains and the quality of a film play a crucial role for the further application. Thus far, many studies[12–21] have been dealing with the aforementioned parameters, but standardization of this technique for utilization in mass production has not been presented yet.

In this article, we conducted the solvent vapor annealing of the well-explored BCP, poly(styrene-b-4-vinylpyridine), using three common solvents: toluene, chloroform, and tetrahydrofuran (THF). Restriction of parameters on static conditions and the saturated pressure of solvents together with an investigation of the kinetics provide only temperature as an elective parameter. The BCPs are exemplary self-assembling systems which have shown a great potential as templates for nanoscale optics and

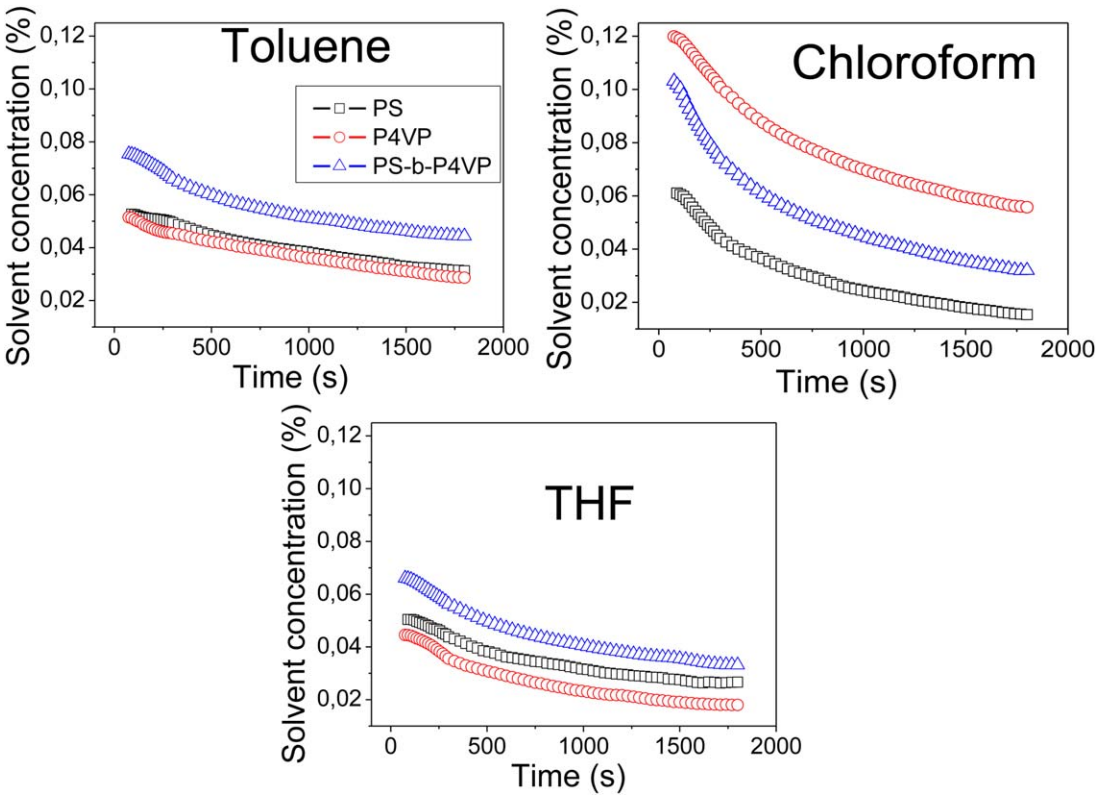


**Figure 1.** Relative solvent loss at ambient conditions after the annealing of PS, P4VP, and PS-b-P4VP (thickness 1 μm). The films were annealed at 50°C for 3 h in the saturated vapors of toluene, chloroform, and THF. [Color figure can be viewed in the online issue, which is available at wileyonlinelibrary.com.]

electronics.[22] As an example, the phase separation can be used for the preparation of highly ordered arrays of metal nanoparticles.[23] Alternatively, ordered BCPs can be applied for the preparation of isoporous membranes for highly selective separation.[24]

## EXPERIMENTAL

### Materials

Polystyrene (PS, $M_w = 150{,}000$ g mol$^{-1}$) and poly(4-vinylpyridine) (P4VP, $M_w = 160{,}000$ g mol$^{-1}$) were purchased from Sigma Aldrich. Poly(styrene-b-4-vinylpyridine) (PS-b-P4VP) was purchased from polymer source. The PS-b-P4VP had following parameters: $M_w/M_n = 1.1$ (PS-b-P4VP); $M_n$ (PS) = 33,000 g mol$^{-1}$; $M_n$ (P4VP) = 8000 g mol$^{-1}$). Toluene, chloroform, tetrahydrofuran (THF), methanol, ethanol, 1,2-dichlorethane were purchased from Sigma Aldrich.

### Methods

About 0.01 g of PS was dissolved in 25 g of toluene, 0.01 g of P4VP and 0.01 PS-b-P4VP were dissolved in 20 g of ethanol and 18 g of 1,2-dichlorethane, respectively. Thin polymer films were deposited by spin-coating (1000 rmp, 60 s) on a glass substrate. After the deposition, the films were dried at ambient conditions for 24 h. Film thickness (cca 50 nm) was controlled by a profilometry and optical measurement (refractometry).

### Annealing Procedure

Films were placed in a vacuum chamber with aliquot of solvents and the chamber was heated to 50°C. Toluene, chloroform, and THF were used as solvents. The quantity of solvents was calculated to reach the saturated vapor value under the set experimental conditions using Van der Waals equation (chamber volume and temperature were taken into account). The amounts of solvents were 0.175 g of toluene, 1.303 g of chloroform, and 0.661 g of THF.

### Surface Reconstruction

The surface reconstruction is the next operation often needed for better ordering and emphasis of the morphology described in the literature.[25,26] The surface reconstruction was done after the phase separation by immersion of the films into ethanol or methanol for 0.5 h. Residual solvents were removed by the stream of nitrogen and films were dried at ambient conditions during 24 h before further measurements.

### Characterization

The solvent desorption tests were performed to estimate the solvent–polymer interaction through a mass-change measurement. For gravimetry tests were prepared thicker samples (1 μm). Samples were placed into the solvent vapor for 3 h and then the time-resolved mass loss was measured *in situ* at the ambient conditions. After the vapor annealing, the samples were purged with a stream of air for 10 s to remove the "surface" solvents.

Kinetics of the phase separation was determined by a refraction spectroscopy. The refraction spectra were taken *in situ* during the annealing in the spectral range 250–750 nm using refractometer Avaspec 2048. In the case of pristine PS, the change of film

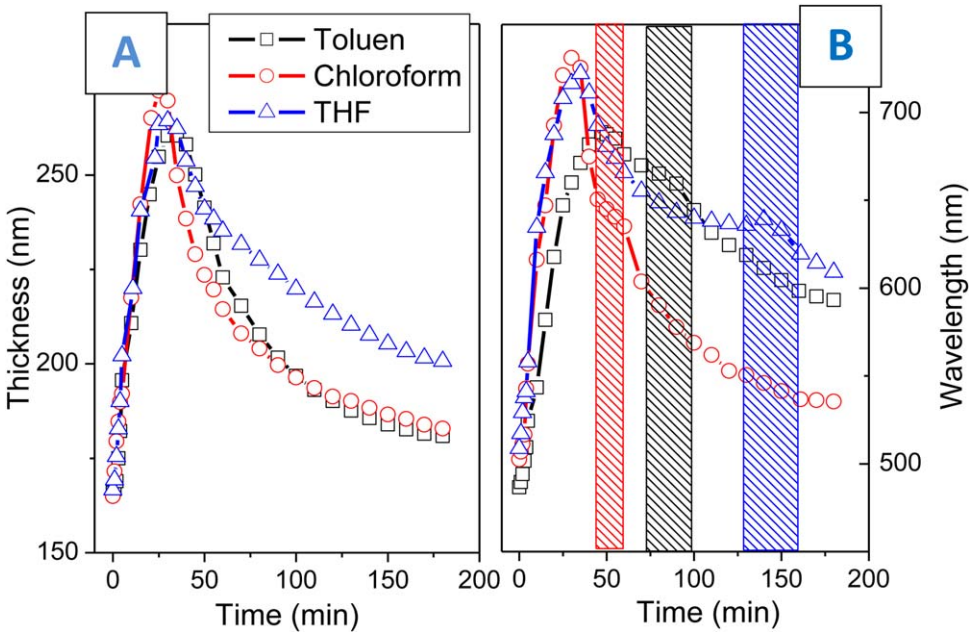


**Figure 2.** Evaluation of the PS thickness (A) and position of interference maximum (B) in the PS-b-P4VP films during the vapor annealing. [Color figure can be viewed in the online issue, which is available at wileyonlinelibrary.com.]

thickness was calculated with the AvaSoft Full 6.1, including code Spectra 3. For PS-b-P4VP directly the wavelength position of the second interference maximum was taken into account.

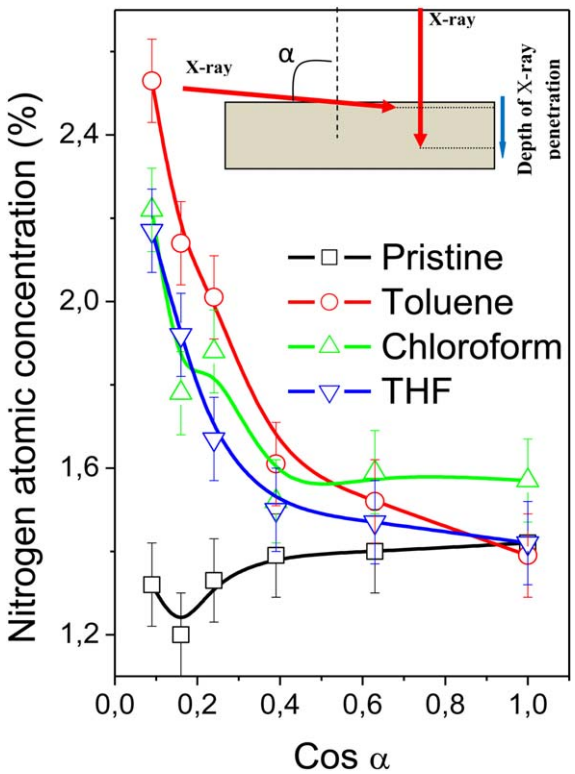


**Figure 3.** Depth profiles of nitrogen concentration in the PS-b-P4VP films before and after the modification (toluene, chloroform, and THF vapor annealing followed by the surface reconstruction). [Color figure can be viewed in the online issue, which is available at wileyonlinelibrary.com.]

The surface morphology was examined by atomic force microscopy (AFM, tapping mode), under ambient conditions on Digital Instruments CP II set up (Veeco). The oxide-sharpened silicon probes RTESPA-CP) were used. The dimension of analyzed areas was 1 × 1 and 0.5 × 0.5 $\mu m^2$. The quality of the BCPs films after solvent treatment and surface reconstruction were studied at microscale dimension using upright laser confocal microscope Olympus Lext working with a 405 nm laser light. For the sample observation an objective lens with 50× magnification was used.

Angle resolved X-ray photoelectron spectroscopy (XPS) were measured by Omicron Nanotechnology ESCAProbeP spectrometer. The focus was on depth profile of nitrogen (1s) concentration. The analyzed area had dimension of 2 × 3 $mm^2$. The concentration of nitrogen was calculated in at. % (error ± 0.1%).

## RESULTS AND DISCUSSION

The solvent affinity under applied experimental conditions and the kinetics of solvent penetration into the polymer films were estimated by gravimetry and *in situ* refractometry measurements. The gravimetry results are presented in Figure 1. Two parameters must be taken into account—the total amount of entrapped solvents and the escape rate of solvents. The amount of entrapped solvent depends on the polymer affinity and solvent vapor pressure (toluene—12.2 KPa, chloroform—70.3 KPa, THF—58.6 KPa). The rate of solvent excluding is determined by the solvent affinity and the solvent concentration in polymer. The amounts of penetrated chloroform were higher in all cases (see Figure 1). This was caused by the high value of chloroform vapor pressure. This phenomenon was more pronounced in the P4VP and slightly less in the PS-b-P4VP films. On the other hand, the decrease of chloroform concentration occurred very quickly especially in the case of PS and PS-b-P4VP and it

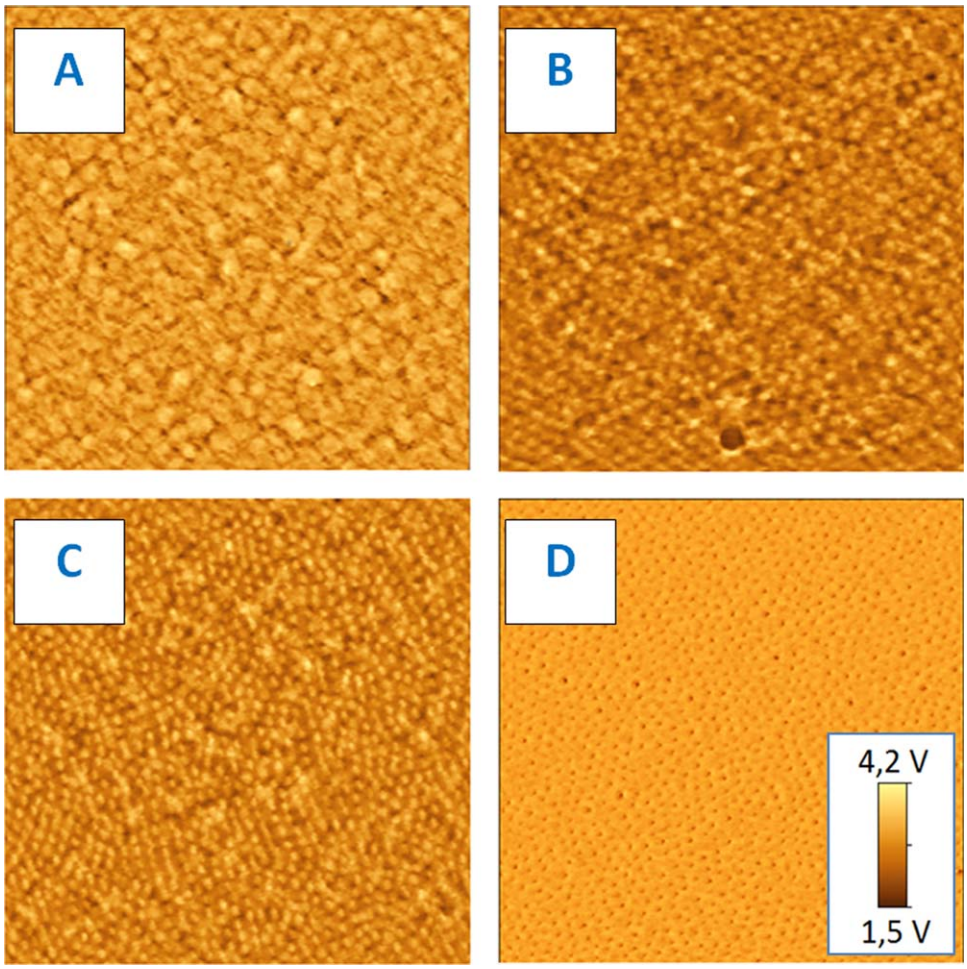


**Figure 4.** Phase AFM scans of the PS-b-P4VP films (thickness 50 nm): (A) before the vapor annealing, (B) after the vapor annealing in THF, (C) after the surface reconstruction in ethanol, and (D) after the surface reconstruction in methanol. [Color figure can be viewed in the online issue, which is available at wileyonlinelibrary.com.]

reflected bad affinities of these polymers to the solvents. The amount of entrapped toluene was slightly higher in the case of PS than in the P4VP films. The escape rates were similar for both polymers. However, the PS-b-P4VP captured apparently much more toluene then pristine polymers. A similar situation was observed in the case of THF. The entrapped amount of the THF and the releasing rate were similar for PS and P4VP, but PS-b-P4VP exhibited more effective capture of THF. Probably, this phenomenon could be attributed to the interphase (mixing) zones in the PS-b-P4VP, where PS and P4VP were simultaneously presented.

The gravimetry results were summarized as follows: under applied experimental conditions chloroform was a good solvent for all discussed polymers, but the highest affinity was to P4PV. Toluene and THF were less sensitive. Toluene was more absorbed. On the other hand, the presence of interphase region in the PS-b-P4VP promoted the capture of THF and toluene and slowed down the release of solvents.

PS is a main domain in PS-b-P4VP, changes of the PS thickness during the annealing were observed and the results are presented in Figure 2(A). Two main areas were evident: the rapid increase of polymer thickness at initial stage and the gradual decrease of thickness under the later treatment. The first region corresponded to the saturation of solvent vapor in the working chamber and solvent capture by the polymer film. Then, the gradual heating of the entire working chamber and polymer films occurred simultaneously with increasing pressure, the solvent was partially released and the thickness of the polymer film decreased. In the solvent sorption/desorption balance, the film thickness tended to reach a constant value. In the case of PS-b-P4VP films, estimation of the film thickness was too complicated because of the presence of two different polymers and the changes of their mutual orientation during the annealing. Thus, the position of the interference maximum in the refraction spectra was used to indicate the PS-b-P4VP separation [Figure 2(B)]. The position of the interference maximum depended on the film thickness and the refractive index. Similar spectra, as in the case of pristine PS could be expected. However, some deviations from the continuous shapes were evident [see Figure 2(B)]. These deviations were depicted by the shaded areas and could be attributed to the phase separation of the PS-

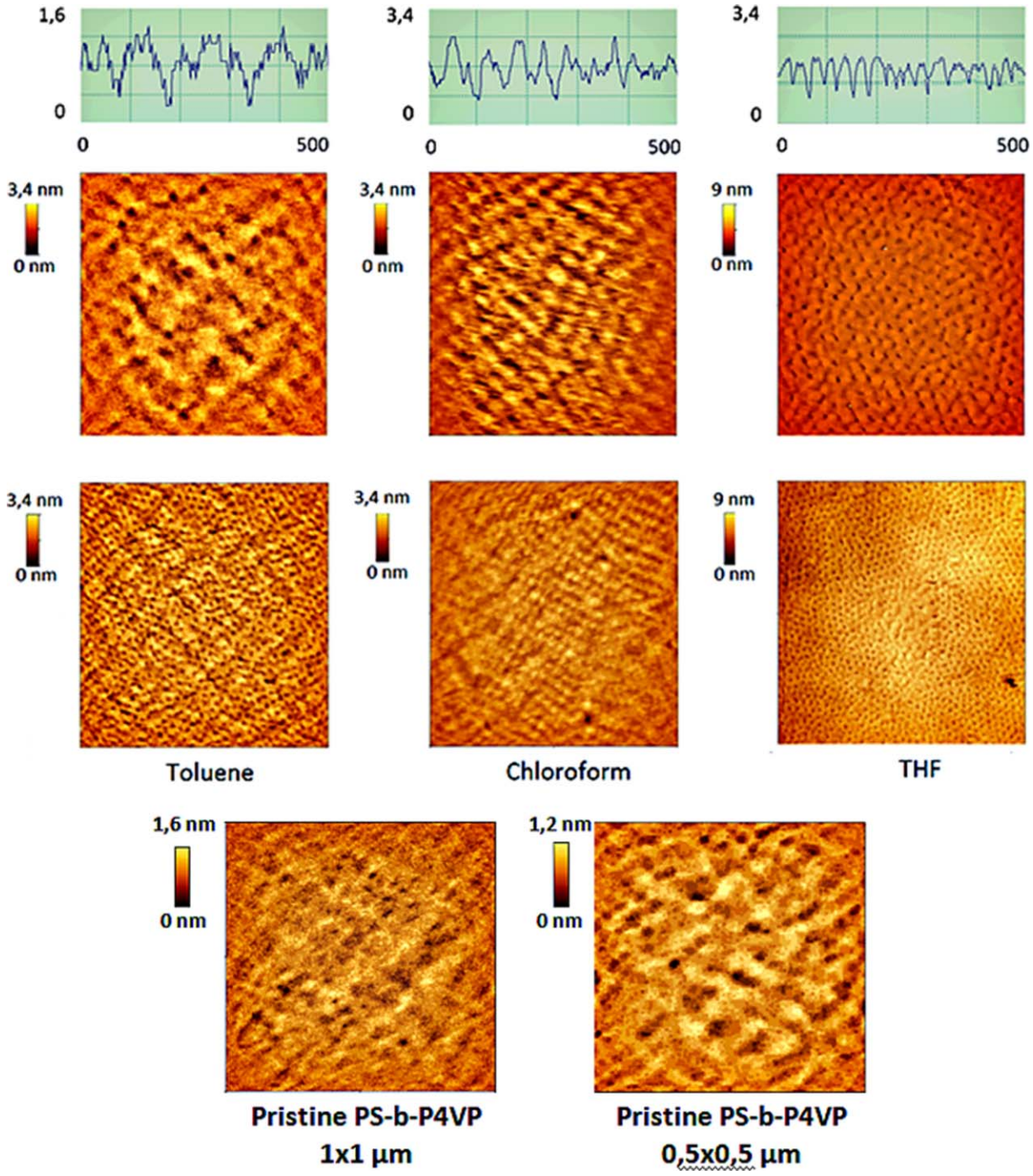


**Figure 5.** AFM images of the 1 × 1 and 0.5 × 0.5 $\mu m^2$ films of PS-b-P4VP (thickness 50 nm) annealed in the saturated vapors of toluene, chloroform, and THF; then exposed to the surface reconstruction in methanol. The top charts show the cross-sectional cut of the surface structure along a horizontal line drawn through the center of the 0.5 × 0.5 µm scans. The pristine films scans are shown at the bottom of the figure. [Color figure can be viewed in the online issue, which is available at wileyonlinelibrary.com.]

b-P4VP. Thus, time intervals of the PS-b-P4VP phase separation could be estimated: chloroform 44–60 min, toluene 73–99 min, and THF 128–159 min. In the case of chloroform, the phase separation began earlier and took the shortest time. In the case of THF, the phase separation began last (after 2 hours) and took almost half an hour.

The BCP films with cylindrical microdomains oriented perpendicularly on the substrate are of particular interest because elimination of the minor component or surface reconstruction in a selective solvent transforms the structures into dots arrays. It was proposed that this process is often accompanied by stretching of the one BCP component on the surface, which leads to

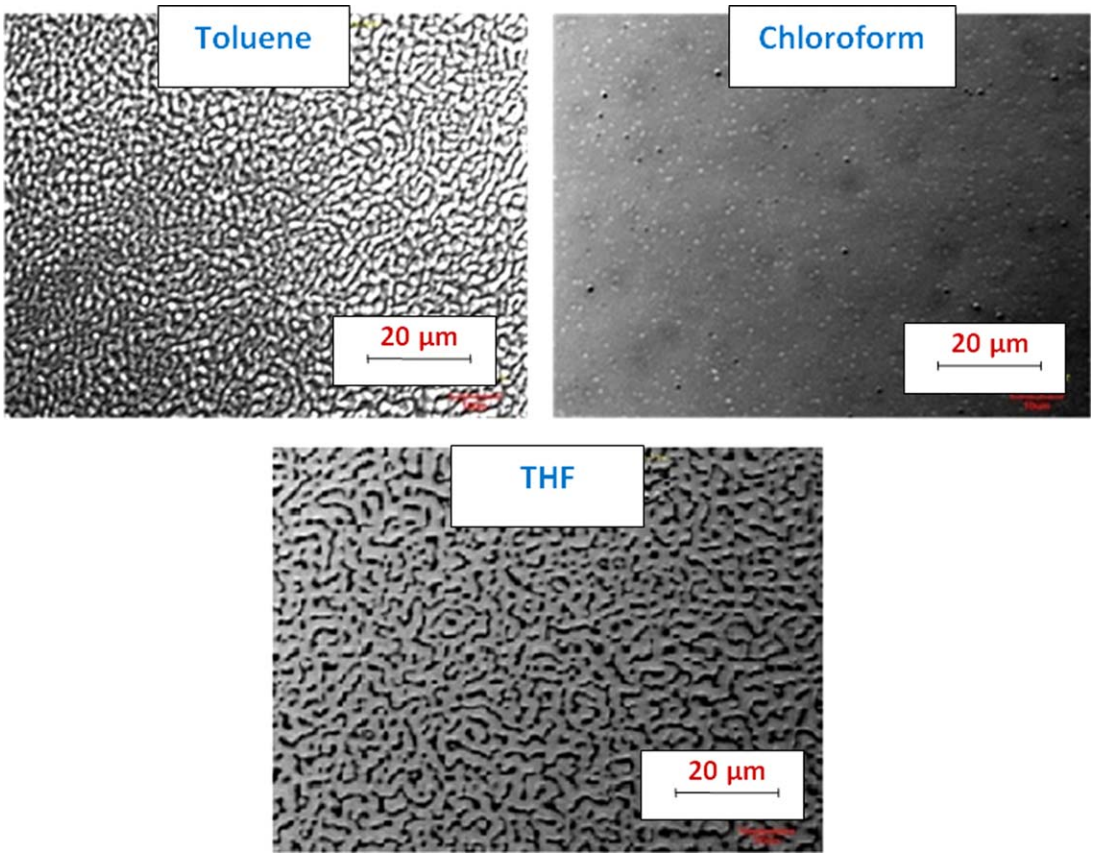


**Figure 6.** Images from the confocal microscope. PS-b-P4VP films (thickness 50 nm) annealed in the saturated vapors of toluene, chloroform, and THF and exposed to the surface reconstruction in methanol. [Color figure can be viewed in the online issue, which is available at wileyonlinelibrary.com.]

changes in surface concentration of the elements. The depth profiles of nitrogen (the characteristic marker of the P4VP block) are given in Figure 3, where results are shown for the PS-b-P4VP before and after the phase separation in toluene, chloroform and THF followed by the surface reconstruction. Insert in Figure 3 gives the physical means of performed experiments: when angle of X-rays incident was close to the surface normal, deeper penetration of radiation occurred and approximately 5 nm thick layer was analyzed. When angle of X-rays incident was close to the surface plane, shallow penetration took place and the signal was collected from less than 0.5 nm thick layer. It was evident, that the nitrogen concentration was approximately constant before the PS-b-P4VP processing (see Figure 3). It could be concluded, that P4VP blocks were homogeneously distributed throughout the film. After the annealing, followed by the surface reconstruction, the near-surface nitrogen concentration achieved apparently higher value. This indicated that during modification the P4VP blocks were stretched on the polymer surface.

The increase of nitrogen concentration on the sample surface occurred independently on solvent used. It has been shown that solvent selectivity for one block of the PS-b-P4VP, which caused stretching of the more soluble component.[21] However, in our case solvent affinity did not affect resulting nitrogen depth profile. So, we proposed that the observed changes appeared during the further processing—surface reconstruction. For verification of this assumption, the AFM phase scans of the samples with reconstructed surface by ethanol or methanol were performed. The results are presented in Figure 4, where the scans show pristine PS-b-P4VP film [Figure 4(A)], annealed PS-b-P4VP film in THF [Figure 4(B)] and PS-b-P4VP film with the reconstructed surface by immersion in ethanol or methanol films [Figure 4(C,D)]. It was evident, that the pristine PS-b-P4VP film had disordered structure where both PS and P4VP were presented on the PS-b-P4VP film surface. After the vapor annealing, ordered structure appeared, but as in the case of pristine PS-b-P4VP film, PS, and P4VP were presented on the film surface. The following surface reconstruction with methanol led to the structure improvement and to the qualitative changes of the surface composition. However, application of methanol led to stretching of the P4VP blocks, which almost completely covered the film surface. When ethanol was used for the surface reconstruction, no stretching occurred. It could be concluded that the changes of surface composition appeared after the surface reconstruction step. Probably, during the surface reconstruction methanol tried to dissolve P4VP completely, but cannot pull it into the solution, because the second part of PS-b-P4VP—PS is insoluble in methanol. After the surface reconstruction completion and methanol removing, P4VP returned to the solid phase and covered the surface of the PS-b-P4VP film. In other words, methanol dissolved the P4VP-part of the film and pulled it onto the surface.

Surface morphology of the PS-b-P4VP films after the surface reconstruction is given in Figure 5. According to the literature the equilibrium morphology of PS-P4VP in bulk is cylindrical.[27] Separation of the individual phases of the PS-b-P4VP films occurred in all cases, however, quality and geometry of the resulted structures was different. It was evident that the worst solvent was toluene. Toluene created semi-ordered hole-structures, the resulted pattern became more pronounced at a higher resolution ($0.5 \times 0.5$ μm$^2$ scan). The use of chloroform led to a "better" result, surface pattern with higher quality at both micro- and nanoscale resolution was observed. According to the AFM, the best results were obtained with the THF annealing. Both, $1 \times 1$ and $0.5 \times 0.5$ μm$^2$ scans exhibited good quality of the surface pattern. For better illustration of the surface features, the depth profile histograms were taken along the horizontal line, in the middle part of the $0.5 \times 0.5$ μm$^2$ scans (Figure 5). The depth profiles confirmed "good" quality of the surface pattern, deviations from the surface plane were periodical with equal amplitude. In the case of toluene and chloroform, the surface features of annealed films were worse. The annealing in toluene led to almost completely impaired surface. The annealing in chloroform resulted in more regular surface features, but the result could not be regarded as the ideal film structure. For comparison, the pristine PS-b-P4VP morphology is also shown in Figure 5. The pristine films had surface with no signs of order. It must be noted that in several studies the phase separation of the PS-P4VP occurred during a spin-coating procedure.[13] It was apparent, that in our case this phenomenon did not occur.

Many self-assembled nanostructures still contain defects and lack a tolerable long-range order for certain nanotechnology applications. The BCPs phase separation usually exhibit only surface morphology measured by AFM technique at local places. The general idea of maintaining the structure of the film in a more general scale, often glossed over. In order to give a more general characteristic of the prepared films, we also made confocal microscopy measurement, obtained results are given in Figure 6. It was evident that the use of toluene and THF dramatically destroyed the film structure. The initially homogeneous films were disrupted into island-like structures. In the case of toluene, such result could be expected: bad solvent, indistinct nanopattern and disrupted film correlated with each other. However, in the case of THF, the images of confocal microscopy are not in agreement with the AFM: good nanopattern, but bad quality of the polymer films. Only in the case of chloroform treatment, preservation of the film structure and good nanopattern were observed.

## CONCLUSION

The phase separation for creation of the block copolymer PS-b-P4VP ordered into nanostructures at elevated temperature and saturated solvent vapor was investigated. THF, chloroform, and toluene were used as solvents. The solvent affinity and the kinetics of solvent penetration into a polymer film were measured gravimetrically and by refractometry. The quality of nanostructures was examined using AFM and confocal microscopy.

Some disagreement between the results from the AFM and confocal microscopy were observed. In the case of toluene application, "poor" nanopattern and disrupted polymer films were observed by both the AFM and confocal microscopy. It the case of THF, "good" nanopattern was found by AFM, but confocal microscopy showed disruption of the polymer films. Chloroform was found to be the most suitable solvent. The use of chloroform led to the formation of satisfactory and homogeneous nanostructures without disruptions. Additionally, chloroform initiated the phase separation fastest, the phase separation began after 45 min of annealing and took 1 h.

## ACKNOWLEDGMENTS

This work has been supported by the Grant Agency of the Czech Republic (No. P108/12/G108).

## REFERENCES

1. Lyutakov, O.; Huttel, I.; Prajzler, V. *J. Polym. Sci. B Polym. Phys.* **2009**, *47*, 1131.
2. Lyutakov, O.; Svorcik, V.; Huttel, I.; Siegel, J.; Kasalkova, N.; Slepicka, P. *J. Mater. Sci. Mater. Electron.* **2008**, *19*, 1064.
3. Somani, R. H.; Hsiao, B. S.; Nogales, A.; Srinivas, S.; Tsou, A. H.; Sics, I.; Balta-Calleja, F. J.; Ezquerra, T. A. *Macromolecules* **2000**, *33*, 9385.
4. Chiche, A.; Stafford, C. M.; Cabral, J. T. *Soft Matter* **2008**, *4*, 2360.
5. Tuma, J.; Lyutakov, O.; Huttel, I.; Slepicka, P.; Svorcik, V. *J. Appl. Phys.* **2013**, *114*, 093104.
6. Schaffer, E.; Harkema, S.; Roerdink, M.; Blossey, R.; Steiner, U. *Macromolecules* **2003**, *36*, 1645.
7. Park, S.; Kim, B.; Yavuzcetin, O.; Tuominen, M. T.; Russell, T. P. *ACS Nano* **2008**, *2*, 1363.
8. Boltau, M.; Walheim, S.; Mlynek, J.; Krausch, G.; Steiner, U. *Nature* **1998**, *391*, 877.
9. Lyutakov, O.; Tuma, J.; Huttel, I.; Prajzler, V.; Siegel, J.; Svorcik, V. *Appl. Phys. B Lasers Opt.* **2013**, *110*, 539.
10. Kim, D. Y.; Li, L.; Jiang, X. L.; Shivshankar, V.; Kumar, J.; Tripathy, S. K. *Macromolecules* **1995**, *28*, 8835.
11. Segalman, R. A. *Mater. Sci. Eng. R* **2005**, *48*, 191.
12. Albert, J. N. L.; Epps, T. H. *Mater. Today* **2010**, *13*, 24.
13. Park, S.; Wang, J. -Y.; Kim, B.; Chen, W.; Russell, T. P. *Macromolecules* **2007**, *40*, 9059.
14. Hahm, J.; Sibener, S. J. *J. Chem. Phys.* **2001**, *114*, 4730.
15. Huang, W. -H.; W. H.; Chen, P. -Y.; Tung, S. -H. *Macromolecules* **2012**, *45*, 1562.
16. O'Driscoll, S.; Demirel, G.; Farrell, R. A.; Fitzgerald, T. G.; O'Mahony, C.; Holmes, J. D.; Morris, M. A. *Polym. Adv. Technol.* **2011**, *22*, 915.
17. Park, S. -Y.; Sul, W. -H.; Chang, Y. -J. *Macromolecules* **2007**, *40*, 3757.
18. Gowd, E. B.; Bohme, M.; Stamm, M. *IOP Conf. Ser. Mater. Sci. Eng.* **2010**, *14*, 012015.
19. Kim, S.; Jeon, G.; Heo, S. W.; Kim, H. J.; Kim, S. B.; Chang, T.; Kim, J. K. *Soft Matter* **2013**, *9*, 5550.

20. Si, H.-Y.; Chen, J.-S.; Chow, G.-M. *Colloids Surf A Physicochem. Eng. Asp.* **2011**, *373*, 82.
21. Zhao, J.; Jiang, S.; Ji, X.; An, L.; Jiang, B. *Polymer* **2005**, *46*, 6513.
22. Di Mauro, A. E.; Villone, V.; Ingrosso, C.; Corricelli, M.; Oria, L.; Perez-Murano, F.; Agostiano, A.; Striccoli, M.; Curri, M. L. *J. Mater. Sci.* **2014**, *49*, 5246.
23. Gowd, E. B.; Nandan, B.; Vyas, M. K.; C Bigall, N.; Eychmuller, A.; Schlorb, H.; Stamm, M. *Nanotechnology* **2009**, *20*, 415302.
24. Peinemann, K.-W.; Abetz, V.; Simon, P. F. W. *Nat. Mater.* **2007**, *6*, 992.
25. Xu, T.; Stevens, J.; Villa, J. A.; Goldbach, J. T.; Guarini, K. W.; Black, C. T.; Hawker, C. J.; Russell, T. P. *Adv. Funct. Mater.* **2003**, *13*, 698.
26. Park, S.; Wang, J.-Y.; Kim, B.; Russell, T. P. *Nano Lett.* **2008**, *8*, 1667.
27. Rahikkala, A.; Soininen, A. J.; Ruokolainen, J.; Mezzenga, R.; Raula, J.; Kaupinnen, E. I. *Soft Matter* **2013**, *9*, 1492.